

Non-iterative solution of the phase retrieval problem using a single diffraction measurement

H. M. Quiney*, G. J. Williams, K. A. Nugent

School of Physics, The University of Melbourne, Victoria 3010, AUSTRALIA

quiney@unimelb.edu.au

Abstract: Coherent diffractive imaging is a method by which iterative methods are employed to recover image information about a finite object from its coherent diffraction pattern. We employ methods borrowed from density functional theory to show that an image can be recovered in a single non-iterative step for a finite sample subject to phase-curved illumination. The result also yields a new approach to quantitative x-ray phase-contrast imaging.

© 2008 Optical Society of America

OCIS codes: (050.1960) Diffraction theory; (100.3010) Image restoration techniques; (100.5070) Phase retrieval; (110.7440) X-ray imaging.

References and links

1. J. W. Miao, P. Charalambous, J. Kirz and D. Sayre, "Extending the methodology of X-ray crystallography to allow imaging of micrometre-sized non-crystalline specimens," *Nature* **400**, 342-344 (1999).
2. J. R. Fienup, "Phase retrieval algorithms- a comparison," *Appl. Opt.*, **21**, 2758-2769 (1982).
3. V. Elser, "Phase retrieval by iterated projections," *J. Opt. Soc. A.* **20**, 40-55 (2003).
4. S. Marchesini, H. He, H. N. Chapman, S. P. Hau-Riege, A. Noy, M. R. Howells, U. Weierstall and J. C. H. Spence, "X-ray image reconstruction from a diffraction pattern alone," *Phys. Rev. B.* **68**, 140101 (2003).
5. D. Shapiro, P. Thibault, T. Beetz, V. Elser, M. Howells, C. Jacobsen, J. Kirz, E. Lima, H. Miao, A. M. Neiman, D. Sayre, "Biological imaging by soft X-ray diffraction microscopy," *Proc. Nat. Acad. Sci.* **102** 15343-15346 (2005).
6. I. K. Robinson, I. A. Vartanyants, G. J. Williams, M. A. Pfeifer and J. A. Pitney, "Reconstruction of the shapes of gold nanocrystals using coherent X-ray diffraction," *Phys. Rev. Lett.* **87**, 195505 (2001).
7. M. A. Pfeifer, G. J. Williams, I. A. Vartanyants, R. Harder, I. K. Robinson, "Three-dimensional mapping of a deformation field inside a nanocrystal," *Nature* **442**, 63-66 (2006).
8. R. Neutze, R. Wouts, D. van der Spoel, E. Weckert and J. Hajdu, "Potential for biomolecular imaging with femtosecond X-ray pulses," *Nature* **406**, 752-757 (2000).
9. H. N. Chapman, A. Barty, M. J. Bogan, S. Boutel, M. Frank, S. P. Hau-Reige, S. Marchesini, B. W. Woods, S. Bajt, W. Henry, Benner, R. A. London, E. Plönjes, M. Kuhlmann, R. Treusch, S. Düsterer, T. Tschentscher, J. R. Schneider, E. Spiller, T. Möller, C. Bostedt, M. Hoener, D. A. Shapiro, K. O. Hodgson, D. van der Spoel, F. Burmeister, M. Bergh, C. Caleman, G. Huldt, M. Seibert, F. R. N. C. Maia, R. W. Lee, A. Szöke, N. Timneanu and J. Hajdu, "Femtosecond diffractive imaging with a soft X-ray free-electron laser," *Nature Physics* **2**, 839-843 (2006).
10. A. Snigirev, I. Snigireva, V. Kohn, S. Kuznetsov and I. Schelokov, "On the possibilities of x-ray phase contrast microimaging by coherent high-energy synchrotron radiation," *Rev. Sci. Instrum.* **66**, 5486-5492 (1995).
11. M. W. Westneat, O. Betz, R. W. Blob, K. Fezzaa, W. J. Cooper, W. K. Lee, "Tracheal respiration in insects visualized with synchrotron X-ray imaging," *Science* **299**, 558-560 (2003).
12. D. Chapman, W. Thomlinson, R. E. Johnston, D. Washburn, E. Pisano, N. Gmur, Z. Zhong, R. Menk, F. Arfelli, D. Sayers, "Diffraction enhanced X-ray imaging," *Phys. Med. Biol.* **42** 2015-2025 (1997).
13. P. Cloetens, W. Ludwig, J. Baruchel, D. van Dyck, J. van Landuyt, J. P. Guigay and M. Schlenker, "Holotomography: quantitative phase tomography with micrometre resolution using hard synchrotron radiation X-rays," *Appl. Phys. Lett.* **75**, 2912-2914 (1999).

14. K. A. Nugent, T. E. Gureyev, D. F. Cookson, D. Paganin, and Z. Barnea, "Quantitative phase imaging using hard X-rays," *Phys. Rev. Lett.* **77**, 2961-2964 (1996).
15. K. A. Nugent, D. Paganin and T. E. Gureyev, "A phase odyssey," *Physics Today* **54**, 27-32 (2001).
16. G. J. Williams, H. M. Quiney, B. B. Dhal, K. A. Nugent, A. G. Peele, D. Paterson and M. D. de Jonge, "Fresnel coherent diffractive imaging," *Phys. Rev. Lett.* **97**, 025506 (2006).
17. D. Sayre, "Some implications of a theorem due to Shannon," *Acta. Cryst.* **5**, 843 (1952).
18. J. Miao, D. Sayre and H. N. Chapman, "Phase retrieval from the magnitude of the Fourier transforms of non-periodic objects," *J. Opt. Soc. Am. A* **15**, 1662-1669 (1998).
19. K. A. Nugent, "X-ray non-interferometric phase imaging: a unified picture," *J. Opt. Soc. Am. A* **24**, 536-547 (2007).
20. M. R. Teague, "Deterministic phase retrieval: a Green's function solution," *J. Opt. Soc. Am.* **73**, 1434-1441 (1983).
21. D. Paganin, *Coherent X-ray Optics* (Oxford University Press, 2005).
22. K. A. Nugent, A. G. Peele, H. N. Chapman and A. P. Mancuso, "Unique phase recovery for nonperiodic objects", *Phys. Rev. Lett.* **91**, 203902 (2003).
23. T. E. Gureyev, A. Roberts and K. A. Nugent., "Partially coherent fields, the transport of intensity equation, and phase uniqueness," *J. Opt. Soc. Am. A*, **12**, 1942-1946 (1995).
24. R. H. T. Bates, "Fourier phase problems are uniquely solvable in more than one dimension. 1: Underlying theory," *Optik* **61**, 247-262 (1982).
25. M. Abramowitz and I. Stegun (eds), *Handbook of Mathematical Functions*, Dover Publications, New York (1970).
26. H. M. Quiney, A. G. Peele, Z. Cai, D. Paterson, K. A. Nugent, "Diffractive imaging of highly focussed X-ray fields," *Nature Physics* **2**, 101-104 (2006).
27. P. Hohenberg and W. Kohn, "Inhomogeneous electron gas," *Phys. Rev. B*, **136**, B864 (1964).
28. D. Paganin, K. A. Nugent, "Noninterferometric phase imaging with partially coherent light," *Phys. Rev. Lett.* **80** 2586-2589 (1998).

Coherent diffractive imaging is a method that has attracted considerable recent attention. It combines a far-field measurement of diffracted data with some *a priori* knowledge of the object, such as its support, to achieve a reconstruction of the complex scattered wave [1]. Iterative procedures of the type proposed by Fienup [2], Elser [3] and others [4] have been used successfully to obtain images of a number of objects from experimental diffraction data, including biological cells [5] and individual nanocrystals [6]. The method has also been used to image the strain fields within a single crystal [7]. In the longer term, coherent diffractive imaging has been identified as an attractive approach to the imaging of single molecules using X-ray free electron lasers [8], and its feasibility has recently been demonstrated using an ultra-violet free electron laser system [9].

The method of X-ray phase-contrast imaging has been emerging as a parallel development, and has found applications in other areas of X-ray imaging. First reported as an incidental observation from third-generation synchrotron sources [10], it has now been extensively applied to a range of problems, often in the context of the imaging of soft-tissues [11] and medical imaging [12]. Importantly, methods have been developed that allow the phase contrast images to be made quantitative using iterative [13] and non-iterative [14] schemes. In all cases, these methods have been based on an understanding of how the wavefield propagates. Indeed, phase-contrast has its origin in the local curvature in the wavefield leading to focusing and defocusing of the light producing observable intensity contrast [15]. The critical role of phase curvature in enabling direct access to phase information has led to the demonstration of a form of coherent diffraction imaging that uses a curved incident wavefield [16].

This article draws together the two areas of X-ray coherent diffractive imaging and X-ray phase-contrast imaging. We explore the theory of X-ray diffraction when an object is illuminated by a spherically expanding beam, providing a connection between the transport of intensity approach to phase contrast imaging and the recovery of image information from coherent diffraction data. Crystallography, coherent diffractive imaging and quantitative phase imaging all share the aim of recovering phase information from intensity data. Crystallography builds

on the periodicity inherent to a crystal and assumes that the data is obtained in the far-zone of the field. Coherent diffractive imaging removes the assumption of periodicity, replacing it with the assumption of finite support. Fresnel coherent diffractive imaging adds the requirement for a phase-curved incident field. Quantitative phase-imaging also uses the Fresnel formalism but removes the assumption of finite support and the far-zone and, in general, adds the need for two measurement planes. It also can recover the image information deterministically.

The complex amplitude of a propagating wave is specified by its phase and amplitude distributions. That is, each point in the wavefield is specified by two real numbers. In general, we need at least $2N$ real numbers to recover a wavefield at N points. For example, two intensity measurements are required to constrain properly an algorithm that seeks to recover the complex amplitude; this is the observation that underpins the “oversampling” argument [17, 18] used in coherent diffractive imaging. An analysis of quantitative phase imaging [19] has sought to classify these techniques on the basis by which adequate information is acquired through *a priori* information about the sample size and shape (its support), its optical properties or by acquiring two or more sets of intensity data. The central idea of the present paper is the suggestion that a fourth approach, based on ideas borrowed from density functional theory, may be used, in which we use *a priori* information about the illumination to enable us to assume a functional form for the propagation of the scattered wave.

Consider quantitative phase imaging using the transport of intensity equation [20, 21]. This approach uses the condition of energy conservation to relate the intensity and phase distributions in a given plane at z , $I(\mathbf{r}, z)$ and $\Phi(\mathbf{r}, z)$ respectively, to the longitudinal intensity derivative in that plane:

$$\nabla_{\perp} \cdot I(\mathbf{r}, z) \nabla_{\perp} \Phi(\mathbf{r}, z) = -\frac{2\pi}{\lambda} \frac{\partial I(\mathbf{r}, z)}{\partial z} \quad (1)$$

where λ is the wavelength and ∇_{\perp} denotes the transverse gradient operator. Apart from crystallography, all of the methods touched on in the previous paragraph adopt the paraxial approximation, an approximation also made here. In practice, an approximation to the derivative on the right hand side of Eq. (1) is formed from intensity measurements made at two closely spaced planes. Provided the intensity is strictly positive over a simply connected region, the phase distribution may be uniquely recovered to within a physically meaningless additive constant [23]. For the far-zone application of this approach to succeed, a curved incident beam is needed to form a Fresnel diffraction pattern. In this far-zone Fresnel diffractive imaging configuration, a derivative with respect to the curvature of the illumination replaces the derivative with respect to propagation [22]. In practice, however, a derivative with respect to changes in the incident wavefield curvature is much harder to acquire and is probably impractical.

In this article we use the structure of the physics of diffraction and the familiar coherent diffractive imaging assumption of finite support to demonstrate that the derivative on the right hand side of Eq (1) may be very well-approximated from a single plane of diffraction data, a conclusion we support via a simple numerical demonstration. This result has two important implications that we explore. First, it opens the way to a non-iterative solution of the coherent diffractive imaging problem, obviating much of the work on the development of complex iterative image recovery algorithms. Secondly it suggests a new approach to quantitative phase imaging that removes the need for two planes of intensity data.

Consider the experimental arrangement sketching in Fig. 1 which is the configuration for Fresnel coherent diffractive imaging. In the paraxial Fresnel diffraction formalism, information about the field in a plane at z_1 is communicated to a plane at z_2 via the expression

$$\psi(\mathbf{r}_2, z_2) = -\frac{i \exp\left(\frac{2\pi i z}{\lambda}\right)}{\lambda Z} \exp\left(\frac{i\pi r_2^2}{\lambda Z}\right) \iint \psi(\mathbf{r}_1, z_1) \exp\left(\frac{i\pi r_1^2}{\lambda Z}\right) \exp\left(-\frac{2\pi i \mathbf{r}_1 \cdot \mathbf{r}_2}{\lambda Z}\right) d\mathbf{r}_1 \quad (2)$$

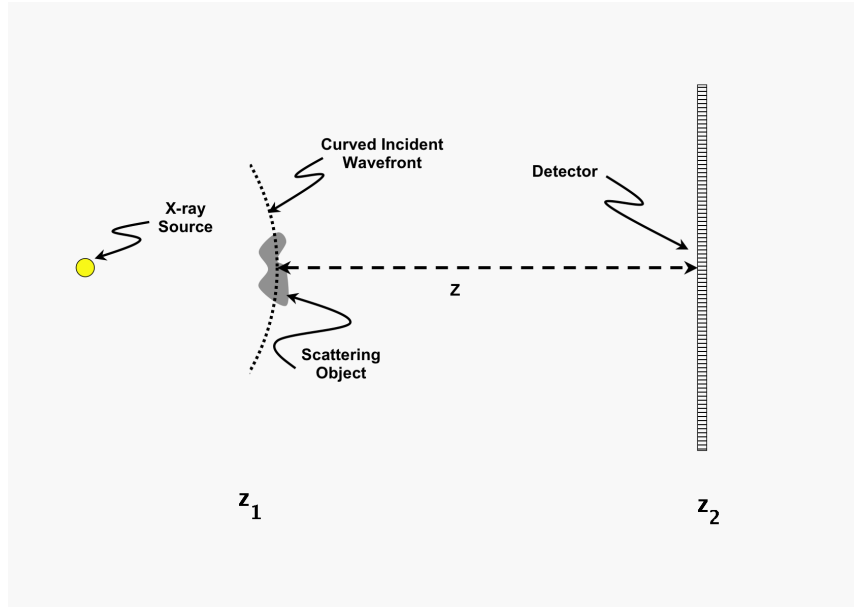


Fig. 1. Schematic representation of the imaging configuration. An X-ray source produces a wavefront that has significant spherical phase curvature in the plane of the diffracting object. The diffracted and undiffracted waves propagate paraxially to a distant plane where they are detected.

where $Z = z_2 - z_1$. We assume that the scattered field at z_1 has finite support and that the detector plane is at z_2 . Our aim is to construct a method by which the intensity data at z_2 can be used to construct an expression for the longitudinal intensity derivative in that plane, thereby allowing a non-iterative phase recovery using Eq. (1).

A useful connection between Eq. (1) and Eq. (2) may be established by defining the function

$$g(\mathbf{w}) = \exp\left(\frac{i\pi w^2}{\lambda Z}\right) \iint_{S(\mathbf{w})} \psi(\mathbf{r}_1 + \mathbf{w}, z_1) \psi^*(\mathbf{r}_1, z_1) \exp\left(\frac{2\pi i \mathbf{r}_1 \cdot \mathbf{w}}{\lambda Z}\right) d\mathbf{r}_1, \quad (3)$$

in which form $g(\mathbf{w})$ may be regarded both as the autocorrelation of $\psi(\mathbf{r}_1, z_1) \exp(i\pi r_1^2 / \lambda Z)$ and the inverse Fourier transform of $I(\mathbf{r}_2, z_2)$. The region of integration, $S(\mathbf{w})$, is specified completely by the support of $\psi(\mathbf{r}_1, z_1)$. We may complete the formal correspondence between Eq. (1) and Eq. (2) if we note that

$$\frac{\partial I(\mathbf{r}_2, z_2)}{\partial z} = \iint_{S(\mathbf{w})} \frac{\partial g(\mathbf{w})}{\partial Z} \exp\left(-\frac{2\pi i \mathbf{w} \cdot \mathbf{r}_2}{\lambda Z}\right) d\mathbf{w} - \frac{1}{Z} \mathbf{r}_2 \cdot \nabla_{\perp} I(\mathbf{r}_2, z). \quad (4)$$

The dilation factor $-(1/Z) \mathbf{r}_2 \cdot \nabla_{\perp} I(\mathbf{r}_2, z_2)$, which is readily constructed from $I(\mathbf{r}_2, z_2)$, isolates the trivial, spherically-expanding component of $I(\mathbf{r}_2, z_2)$, and the partial derivative of $g(\mathbf{w})$ is taken with respect to Z because the source plane at z_1 is regarded as fixed. Since $\psi(\mathbf{r}_1, z_1)$ and $S(\mathbf{w})$ are independent of Z , then an application of Leibnitz' Theorem [25, Eq. 3.3.7] yields

$$\frac{\partial g(\mathbf{w})}{\partial Z} = -\frac{i\pi w^2}{\lambda Z^2} g(\mathbf{w}) - \frac{2\pi i}{\lambda Z^2} \exp\left(\frac{i\pi w^2}{\lambda Z}\right) \iint_{S(\mathbf{w})} \mathbf{w} \cdot \mathbf{r}_1 \psi(\mathbf{r}_1 + \mathbf{w}, z_1) \psi^*(\mathbf{r}_1, z_1) \exp\left(\frac{2\pi i \mathbf{r}_1 \cdot \mathbf{w}}{\lambda Z}\right) d\mathbf{r}_1. \quad (5)$$

This is readily transformed into a form more accessible to physical interpretation by a further application of Leibnitz' Theorem

$$\begin{aligned} \frac{\partial g(\mathbf{w})}{\partial Z} = & -\frac{1}{Z}\mathbf{w}\cdot\nabla_{\perp}g(\mathbf{w}) + \frac{i\pi w^2}{\lambda Z^2}g(\mathbf{w}) \\ & -\frac{2\pi i}{\lambda Z^2}\exp\left(\frac{i\pi w^2}{\lambda Z}\right)\iint_{S(\mathbf{w})}\psi^*(\mathbf{r}_1, z_1)\exp\left(\frac{2\pi i\mathbf{r}_1\cdot\mathbf{w}}{\lambda Z}\right)\mathbf{w}\cdot\nabla_{\perp}\psi(\mathbf{r}_1 + \mathbf{w}, z_1)d\mathbf{r}_1 \\ & +T[S(\mathbf{w}), \psi(\mathbf{r}_1, z_1), \mathbf{w}, Z]. \end{aligned} \quad (6)$$

This expression introduces a boundary term, $T[S(\mathbf{w}), \psi(\mathbf{r}_1, z_1), \mathbf{w}, Z]$, whose form is generally too complicated to be written explicitly, but which is defined precisely by Leibnitz' Theorem through the gradient of the boundary that encloses $S(\mathbf{w})$, and the value of the integrand of $g(\mathbf{w})$ on the interior of that boundary. The first two terms in Eq. (6) are readily obtained by direct manipulation of $I(\mathbf{r}_2, z_2)$. The third term is sensitive to the gradient of the wavefield and vanishes identically if, for example, the wavefield is detected at a propagation distance Z from a uniformly illuminated aperture of any exterior shape. Similarly, this term vanishes identically in far-field Fresnel diffraction if such an aperture is illuminated by light possessing constant amplitude and a radius of spherical illumination of Z . The fourth term, $T[S(\mathbf{w}), \psi(\mathbf{r}_1, z_1), \mathbf{w}, Z]$, depends on the exterior shape of $S(\mathbf{w})$, and on the value of $\psi(\mathbf{r}_1, z_1)$ along the edges of $S(\mathbf{w})$. This term vanishes identically if $\psi(\mathbf{r}_1, z_1)$ also vanishes everywhere along the boundaries that define its support, a situation that is readily realized in practice. In general, the third term determines the analytic variation of $\psi(\mathbf{r}_1, z_1)$ within the interior of the object support, while the fourth term fixes $\psi(\mathbf{r}_1, z_1)$ on the edges of the support.

Consider an experimental situation in which we know that the boundary term $T[S(\mathbf{w}), \psi(\mathbf{r}_1, z_1), \mathbf{w}, Z]$ in Eq. (6) is negligible, which will be realised if the edges of the object fall smoothly to zero without jump discontinuities. The resulting coherent diffractive imaging problem is then posed as the solution of an integral equation. The left-hand side and the first two terms on the right hand side are known from the experimental data, since $g(\mathbf{w})$ can be recovered from the measured data by a Fourier transformation. The third term on the right hand side, however, contains the wavefunction to be determined. To deal with this issue we take a perturbative approach and write

$$\psi(\mathbf{r}, z) = \psi_0(\mathbf{r}, z) + \varepsilon\psi_S(\mathbf{r}, z), \quad (7)$$

in which ε is a parameter that we may adjust to change the strength of the perturbation relative to $\psi_0(\mathbf{r}, z)$. It is not a parameter that plays any part in the solution algorithm, and is introduced here only to explore the limits of validity of the scheme as a function of the strength of the perturbation. In all cases of practical interest, the scattered wave, $\psi_S(\mathbf{r}, z)$, is very weak compared to the incident wave, $\psi_0(\mathbf{r}, z)$, and so it is safe to assume that $\varepsilon|\psi_S(\mathbf{r}, z)| \ll |\psi_0(\mathbf{r}, z)|$ for $|\varepsilon| \leq 1$. We also assume that the field incident on the scattering object has been fully characterized by some independent means, such as those described in [26].

In order to circumvent the need to know the wavefield in the construction of the third term in Eq. (6), we now draw on an analogy with the first Hohenberg-Kohn theorem of density functional theory [27]. This theorem states that electron density uniquely specifies the ground state of an electronic system, including its quantum mechanical wavefunction and all its derived properties. In imaging applications, we routinely assume the existence of a unique mapping between a properly sampled optical intensity and all of the properties of the system, but we do so by explicit intermediate construction of a complex wavefield through the resolution of its phase distribution. In order to adopt a strategy in imaging applications that is more closely analogous to that taken in density functional approaches, we need to establish the functional dependence

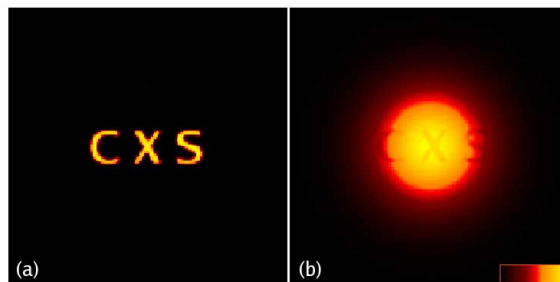


Fig. 2. (a) Diffracting object used in the numerical work. The object is purely real and transmits 10% of the incident intensity. (b) The amplitude of the wavefield leaving the object. The illuminating field is Gaussian in amplitude and has a Fresnel number of 6 over the horizontal dimension of the object.

of $\partial I/\partial z$ on I in the plane of the detector, which is sufficient information from which to derive all optical properties of the system through Eq. (1). Since we assume that $\varepsilon|\psi_S(\mathbf{r}, z)| \ll \psi_0(\mathbf{r}, z)$, we adopt a strategy employed in density functional theory and assume that the functional dependence of $\partial I/\partial z$ on I for the illuminating field, $\psi_0(\mathbf{r}, z)$, remains valid for the perturbed field, $\psi(\mathbf{r}, z)$. This approach is analogous to the use of the free-electron gas model in the specification of an effective zero-order model for the electrostatic exchange potential in density functional theory, which depends only on the electron density.

To illustrate this approach, we consider an object illuminated with an axially aligned Gaussian beam, $\psi_0(\mathbf{r}, z_1) = \exp(-\mu r^2)$, where the real part of μ is positive. In this case, it is straightforward to obtain the explicit functional relationship for the illuminating beam

$$\frac{\partial I_0}{\partial z} = -\frac{\mu}{Z} \iint w^2 g_0(\mathbf{w}) \exp\left(\frac{2\pi i \mathbf{w} \cdot \mathbf{r}}{\lambda Z}\right) d\mathbf{w} \quad (8)$$

where $g_0(\mathbf{w})$ is the Fourier transform of I_0 . This establishes the exact functional relationship between $\partial I_0/\partial z$ and I_0 without making explicit reference to $\psi(\mathbf{r})$ in any plane. The essence of our approach is to use the functional form of Eq. (8) with the experimental measurement of $g(\mathbf{w})$ to devise an estimate of $\partial I/\partial z$.

We now consider the case where this Gaussian beam illuminates a weakly scattering sample, Fig. 2(a), producing the exit wave shown in Fig. 2(b). The far-zone intensity is measured, Fig. 3, and the function $g(\mathbf{w})$ is formed from it by a Fourier transformation.

We substitute these perturbed data into the same functional form of Eq. (8) to form the intensity derivative at the detector plane, Fig. 4(a). This compares extremely well to the exact result, Fig. 4(b). These data are then substituted into the transport of intensity equation and solved for the phase using standard methods of phase retrieval, yielding Fig. 5(a). The recovered phase of $\psi_S(\mathbf{r}_1, z_1)$ is very close to the input phase, a constant, over the region where the amplitude differs significantly from zero. Some artifacts are visible in Fig. 5(a) which have an intensity of less than 5% of the maximum of $\psi_S(\mathbf{r}_1, z_1)$. These are due both to the use of Eq. (8) to calculate $\partial I/\partial z$ for the perturbed wave, as well as numerical errors inherent in the method used to solve Eq. (1) [28]. This sequence of steps provides a rather stringent test of the method, since the perturbation parameter, ε , has been set at 0.1, corresponding to attenuation of the incident amplitude by 10%. The smaller this parameter, the more closely the approximate solution approaches the exact solution, subject to the approximations inherent in the computational method used to solve Eq. (1).

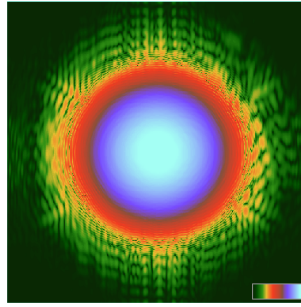


Fig. 3. Logarithmic representation of the far-zone diffraction pattern for the exit wave.

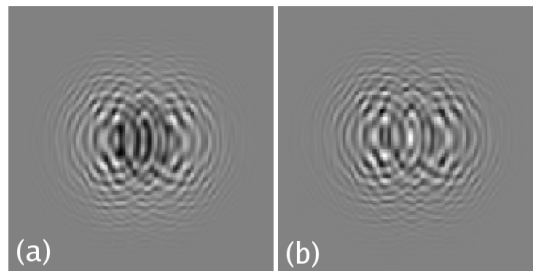


Fig. 4. (a) Approximate far-zone intensity derivative distribution (b) Exact far-zone intensity derivative distribution.

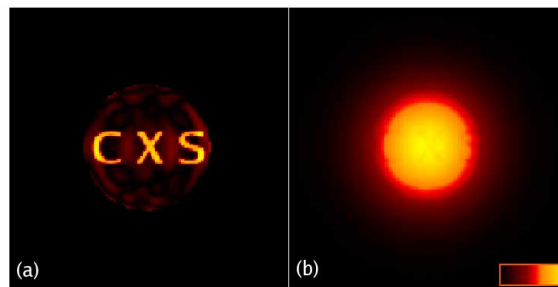


Fig. 5. Non-iterative reconstruction of the diffracting object (a) and exit surface wave (b) using the scheme derived here. The reconstruction is not perfect but represents an excellent starting point for further iterative refinement.

Note that the success of the method depends on the assumption that the scattering function introduces no new terms of the form $T[S(\mathbf{w}), \psi(\mathbf{r}_1, z_1), \mathbf{w}, Z]$ in Eq. (6), which in practice means that the scattered function contains no piecewise discontinuities in the source plane. Consequently, we have constructed the test sample so that its edges are sufficiently smooth that no new edge contributions are introduced into the functional relationship between $\partial I_0/\partial z$ and I_0 . In this case, the transfer function in the scattering plane remains smooth and of small amplitude relative to the incident beam, and the functional relation defined by Eq. (8) is sufficiently close to the exact form so as to provide an accurate solution of the phase problem. In Fresnel diffractive imaging we are always able to recover the illuminating wavefield from measured intensity data [26], which facilitates the construction of the explicit functional relationship involving $\partial I_0/\partial z$ and I_0 that is required in this phase retrieval scheme.

The method described here is, however, necessarily approximate, since one cannot hope to derive an explicit functional relationship between I and $\partial I/\partial z$ in all cases. Indeed, the forms of the functional relations differ markedly from case to case, mainly because of the strong influence of edge effects. The results display a high level of accuracy, and the results may be used to seed refinement by iterative methods. The only restriction that must be observed strictly in practice is that the amplitude of the perturbing wave fall smoothly to zero on its boundary; the wave may be real or complex, subject to this restriction. Iterative methods are necessarily more general, and more stable, because they are not subject to the restrictions inherent in the present algorithm. They are, however, subject to iterative stagnation, and like all non-linear iterative procedures are most useful when the iterative refinement is initiated in the neighbourhood of a solution.

The work described here forms a link between quantitative phase imaging and coherent diffractive imaging. In our introductory comments we did not consider the relationship with holography. While this relationship could be productively explored in more detail, we point out here that the defining feature of holography is its use of a reference wave. Examination of Fig. 3 reveals that much of the diffracted signal in this example falls on the detector in regions in which the undiffracted illumination wave (the reference wave in a holographic interpretation) is negligible or absent. The phase in the region where there is no reference wave could not be recovered using holography, and there would be no prospect of achieving the very high resolution that is the goal of coherent diffractive imaging.

In summary, we have shown that it is possible to obtain a non-iterative solution to the coherent diffractive imaging problem in the case where the incident illumination has a curved wavefront and known intensity profile. We have presented a numerical example that has been constructed to mimic our recent experimental work in Fresnel diffractive imaging [16, 26]. The approach indicates a substantially more reliable approach to the recovery of image information from diffraction data from objects such as single molecules, as has been proposed recently through the use of X-ray free-electron laser sources, as well as the potential for an experimentally simpler approach to phase contrast imaging.

The authors acknowledge valuable discussions with Andrew Peele and support from the Australian Research Council.